Solvation Dynamics of Large van der Waals Aniline−Arn Clusters: Experiment and Theory

ARTICLE *in* THE JOURNAL OF PHYSICAL CHEMISTRY A · AUGUST 2004

Impact Factor: 2.69 · DOI: 10.1021/jp048217t

4 AUTHORS, INCLUDING:

Thomas Pino
Université Paris-Sud 11
83 PUBLICATIONS **856** CITATIONS
SEE PROFILE

Pascal Parneix
Université Paris-Sud 11
76 PUBLICATIONS **874** CITATIONS
SEE PROFILE

Stéphane Douin
Université Paris-Sud 11
41 PUBLICATIONS **390** CITATIONS
SEE PROFILE

Solvation Dynamics of Large van der Waals Aniline−Ar_n Clusters: Experiment and Theory

T. Pino, P. Parneix, S. Douin, and Ph. Bréchignac*

Laboratoire de Photophysique Moléculaire,† CNRS, Fédération de Recherche Lumière Matière, Bât. 210, Université Paris-Sud, F-91405 Orsay Cedex, France

Received: April 23, 2004; In Final Form: June 29, 2004

An experimental and theoretical study of large van der Waals aniline−Ar_n clusters ($n = 7-35$) has been carried out. The van der Waals shift of the $S_1 \leftarrow S_0$ electronic transition and of the vertical ionization potential have been recorded by mass-resolved resonant two-photon two-color ionization techniques. Minimum energy configurations and isomerization processes have been investigated by molecular dynamics simulations. In particular, a careful analysis of the solvation structures at temperatures close to the experimental conditions has been performed by using appropriate global geometrical parameters. This approach allows a deep understanding of the evolution with size arising from the spectroscopic data. A new interpretation of the magic character of the aniline−Ar_{22} cluster observed in the resonant two-photon ionization mass spectrum is proposed.

I. Introduction

Cluster chemical physics focuses on the structure, the isomer stereochemistry, the spectroscopy, and the internal dynamics of large finite size systems at the molecular level. In mixed molecular clusters, the building-up of solvation shells and isomerization between structural conformers are important issues to understand the relationship to condensed phase behavior.[1] Among these systems the structure and dynamics of aromatic−$(solvent)_n$ clusters have been deeply studied in the past decades.[2] The role of the geometry of the cluster, i.e. the local arrangement of the solvent atoms or molecules around the chromophore, has been deeply studied from spectroscopic interrogation in supersonic molecular beam. For small clusters, different conformers have been generally inferred. For the size range involving only a few solvent units the temperature is usually low enough to probe selectively the cluster in a given frozen structure, the spectroscopic features being sharp bands. For larger clusters most of the observations revealed broad bands, where the broadening can be inhomogeneous (numerous isomeric structures) and homogeneous (temperature effect).[3,4] Most of the time, the analyses of the spectroscopic data were done as extensions of those applied on smaller clusters, i.e. using zero-temperature structures. However, clusters prepared in a molecular beam are sampled at a finite nonzero temperature resulting from evaporative cooling. A typical temperature is expected to be about 25 K for an intermediate size (typically 20−30 Ar atoms in interaction with a molecular chromophore) weakly bound van der Waals (vdW) cluster. Thus, because the number of isomers becomes rapidly very large as the size increases, analysis considering only the most stable isomers becomes rapidly inappropriate for large clusters although taking into account the local arrangement of the solvent atoms is still pertinent. To understand such solvation effects at nonzero temperature, we need to analyze "on the fly" the averaged structure from global geometrical parameters adapted for the pertinent description of the system. This "averaged" geometry can be viewed either as the result of many isomers which do not communicate together or as the result of the isomerization dynamics if the temperature is high enough. Thus a temperature effect has to be generally considered.

To investigate the role of the vibrational dynamics at a finite temperature, the aniline−Ar_n clusters appear as excellent candidates in the sense that the vdW electronic shift has been found to be strongly dependent on the specific localization of the Ar atoms relative to the frame of the aniline chromophore.[5−11] Due to the presence of the amino group the solute−solvent interaction of the Ar atoms with the π electrons of the ring is very different from that of the Ar atoms with the substituent. Up to $n = 6$, the vdW electronic shift of the first electronic transition was linked to well-defined binding sites of Ar atoms around the aniline (quasiplanar) chromophore.[10] Analysis of vdW shift for larger clusters could shed light on the spatial localization of the Ar atoms around the aniline molecule and thus the isomerization dynamics. This would enable the understanding of the interplay between the solute−solvent and solvent−solvent interactions, which play an important role in the dynamics of such large clusters.

In addition a possible change of geometry between neutral and ionic clusters is a central question. It is well-known that strong conformational changes occur between the neutral and ionic clusters in the case of phenol/amonia,[12,13] benzene/water,[14−16] and others.[17−19] IR spectroscopic studies have been performed directly in the cationic $(aniline-Ar_n)^+$ in which ions were prepared by photonic excitations.[20−22] In the work of Nakanaga et al.,[20,22] the N−H intramolecular stretching mode frequency was measured as a function of the number of Ar atoms. Recently Solcà and Dopfer[23] have ionized the aniline−Ar and aniline−Ar_2 clusters by an electron impact ion source that enabled the preparation of the cluster ions in their most stable configuration. On the basis of this experimental and theoretical work, they have shown that the most stable structure of the small aniline−Ar_n ($n = 1$ and 2) is not the same for the neutral and ionized clusters. Although the Ar atom is preferentially located above the center of the aromatic ring in the aniline−Ar neutral (forming a π-bound cluster), it was shown

* Address correspondence to this author.
† Laboratoire associé à l'Université de Paris-Sud.

10.1021/jp048217t CCC: $27.50
Published on Web 08/05/2004

that the most stable configuration of the cationic complex is obtained when the Ar atom interacts preferentially with the amino group (so-called H-bound cluster).[23] Therefore even in such weakly bound vdW systems geometrical changes have to be taken care of to interpret spectroscopic data in large clusters.

In the present paper, we will focus on the solvation dynamics in the neutral clusters whose size ranges between 7 and 35, and its possible relationship with the "magic" number $n = 22$. In section II, the experimental setup and procedure are briefly described. In section III, the classical molecular dynamics simulations are presented in details. The experimental results are given in section IV, while section V is devoted to description of the theoretical results, which provide the basis for the general discussion.

II. Experimental Section

The experimental studies of the aniline−Ar_n vdW clusters have been realized in the ICARE apparatus. It consists of a supersonic molecular beam coupled with a 300 mm long linear time-of-flight (TOF) mass spectrometer.[24] The clusters were generated in a supersonic expansion of a gas mixture (An:Ar: He or An:Ar) through a 0.9 mm i.d. pulsed nozzle (opening time $\approx$ 200 μs). The backing pressure was $\approx$5 bar. The molecular beam was extracted through the aperture of a 1 mm diameter conical skimmer before entering the extraction region of the TOF. Aniline−Ar_n clusters were easily produced and measured up to $n \approx 50$. The mass spectra were obtained with a mass resolution of about 300 (at $m = 200$ amu).

The resonant two-photon two-color ionization (R2P2CI) technique has been used. A pulsed frequency-doubled Nd:YAG laser was used to pump a dye laser that was subsequently frequency-doubled to provide a beam of tunable wavelength near $\lambda_1 \simeq 294$ nm. To minimize resonant two-photon one-color ionization, the energy per pulse was carefully adjusted. The second photon was generated by an Excimer laser pumped dye laser operated in the $\lambda_2 = 360-402$ nm wavelength range. By scanning the energy of the first photon (λ_1), the spectra of the $S_1 \leftarrow S_0$ electronic transition origin was recorded. By scanning the energy of the second photon (λ_2) ionization efficiency curves were obtained, which allowed the determination of the vertical ionization potentials (IP).

III. Methodology and Numerical Procedure

The dynamics of the aniline−Ar_n neutral clusters has been investigated in their ground electronic state by molecular dynamics (MD) simulations. During the classical trajectories, the aniline chromophore has been kept as a rigid body. This is generally adopted in such aromatic−rare gas systems due to the large difference between the intra- and intermolecular vibrational frequencies. The potential energy surface (PES) has been built from the sum of the pairwise atom−atom potentials and all the potential parameters can be found in a previous publication.[6] The rotation of aniline was described by the usual quaternion formalism[25] and the classical equations of motion were integrated by using a fifth and fourth order Adams−Moulton predictor−corrector algorithm for the translational and rotational degrees of freedom, respectively. The time integration step was equal to 2 fs and the energy conservation was typically better than 10^{-5}. The total angular momentum of the clusters was taken equal to zero.

The solidlike or liquidlike behavior of a cluster is linked to its ability to vibrate around one given equilibrium geometry or to visit a large number of local minima in the PES. Therefore the analysis of the interatomic distance fluctuations provides information on the rigidity of the vdW cluster. As the cluster is not homogeneous but composed of a chromophore solvated by argon atoms, two different parameters can be calculated. The first one, δ_{Ar-Ar}, is an indicator of the amplitude of the Ar−Ar distances fluctuations:

$$\delta_{Ar-Ar} = \frac{2}{n(n-1)} \sum_{i=1}^{n} \sum_{j>i} \frac{\sqrt{\langle r_{ij}^2 \rangle - \langle r_{ij} \rangle^2}}{\langle r_{ij} \rangle} \tag{1}$$

where r_{ij} corresponds to the distance between the ith and the jth Ar atoms. The second one, δ_{An-Ar}, is related to the rigidity of the Ar_n cluster with respect to the aniline chromophore:

$$\delta_{An-Ar} = \frac{1}{n} \sum_{i=1}^{n} \frac{\sqrt{\langle r_i^2 \rangle - \langle r_i \rangle^2}}{\langle r_i \rangle} \tag{2}$$

where r_i corresponds to the distance between the ith Ar atom and the center of mass of the aniline molecule. In these two equations, the notation $\langle ... \rangle$ indicates a time-averaged value along a microcanonical trajectory.

Following the Lindemann criterion,[26] the cluster exhibits a liquidlike behavior when δ_{Ar-Ar} and δ_{An-Ar} are larger than 0.1. By analyzing the evolution of these two parameters as a function of the internal energy, the melting temperature can be evaluated by using the definition of the kinetic temperature T:

$$T = \frac{2\langle E_k \rangle}{g k_B} \tag{3}$$

where $\langle E_k \rangle$ is the time-averaged kinetic energy, k_B is the Boltzmann constant, and g ($=3n$) corresponds to the number of degrees of freedom of the nonrotating aniline−Ar_n cluster.

However, these parameters give no information about the detailed localization of the Ar atoms around the rather extended aniline molecule. Indeed this chromophore is highly anisotropic in character, first because of its nearly planar structure, and second because the presence of the amino group makes the chemical interaction very different at both ends of the molecule. Actually it was shown that the electronic properties ($S_1 \leftarrow S_0$ electronic transition and ionization potential) are very sensitive to the local positions of the Ar atoms in the vicinity of the aniline molecule.[10] It is therefore interesting to characterize the instantaneous positions of the Ar atoms with respect to the molecular frame along the microcanonical trajectories. Three parameters (S_x, S_y, and S_z) have been calculated:

$$S_\alpha = \sum_{i=1}^{n} \alpha_i \tag{4}$$

in which α_i corresponds to the x_i, y_i, and z_i Cartesian coordinates of the ith Ar atom in the molecular frame. The z-axis is perpendicular to the aromatic plane and the x-axis corresponds to the C−N axis.

All the information about the isomerization dynamics has been extracted from MD simulations for durations larger than 200 ns. In such large vdW systems, local minima are very numerous. An extensive quenching procedure has been realized to find the most stable isomer but also to extract the statistical information about these local minima which play a major role in the dynamics of the cluster in the range of temperatures relevant to experimental conditions. For this purpose, 7000

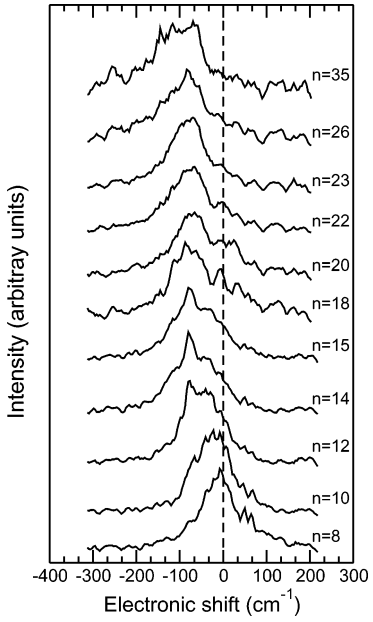

Figure 1. $S_1 \leftarrow S_0$ electronic spectra of aniline$-Ar_n$ clusters, $n = 8-35$, obtained by resonant two-photon two-color ionization. Only a selection of sizes is shown. The center of the wavenumber scale corresponds to the electronic transition in the monomer, identified by the vertical dashed line.

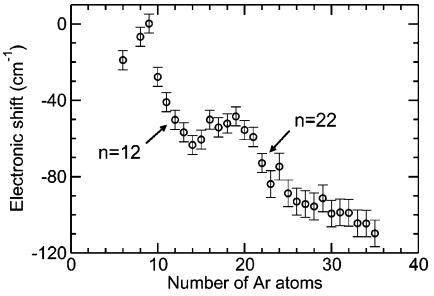

Figure 2. van der Waals electronic shift of the $S_1 \leftarrow S_0$ electronic transition as a function of n, for $n = 6$ to 35. The origin corresponds to the electronic transition in the monomer. The $n = 7$ cluster could not be considered because of the superimposition of the aniline$-Ar_7$ and the $(aniline)_4$ peaks. The wavenumbers were obtained from calculation of the first moment of each spectrum.

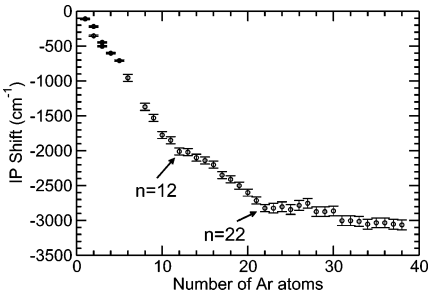

Figure 3. Electronic shift of the vertical ionization potential as a function of n for $n = 1$ to 38. The origin corresponds to the adiabatic ionization potential of the aniline monomer. Up to $n = 6$ data are taken from ref 10.

quenches have been performed for each cluster size every 10 ps along an initial trajectory.

IV. Experimental Results

A. Electronic Spectroscopy. The R2P2CI spectra of the $S_1 \leftarrow S_0$ electronic transition were recorded for $n = 6-35$. A comprehensive sample of these spectra are plotted in Figure 1. To minimize the excess energy deposited in the ions, the spectra were recorded at two different energies of the second photon. In the first case, $h\nu_2$ was fixed just above the ionization threshold of the aniline$-Ar_6$[10] cluster ion giving a maximum excess of energy of about 1300 cm^{-1} in the aniline$-Ar_{15}$ cluster ion. In the second case, $h\nu_2$ was fixed just above the ionization threshold of the aniline$-Ar_{15}$ cluster ion giving a maximum excess of energy of about 1000 cm^{-1} in the aniline$-Ar_{35}$ cluster ion. It was checked that for $n = 15$ and a few masses above, the measured spectra were found to be similar by using the two different second color settings. The first moments of these spectra associated with the origin bands have been extracted from $n = 6$ to 35 and their shift in position relative to the monomer is plotted in Figure 2.

The most striking feature emerging from these patterns is that the spectra are broad band in character, as opposed to the case of smaller clusters ($n = 1-6$) which were exhibiting sharp features.[5,6,10] The characteristic bandwidth (second moment) is about 70 cm^{-1}. Moreover the magnitude of their shift in position relative to the monomer origin band is rather weak. This shift is of the order of that observed for chromophores such as benzene,[27] fluorene,[28] and naphthalene[29] but much smaller than that observed for carbazole,[3] perylene,[30] and dichloroanthracene.[31] Whatever these aromatic$-(rare\ gas)_n$ systems, the electronic vdW shift for $n \approx 25$ is found comparable to that measured in rare gas matrixes. In the case of the aniline molecule, the Ar matrix shift is equal to -114 cm^{-1},[32] which is close to the electronic shift for clusters larger than $n \approx 30$.

The vdW shift of the aniline$-Ar_n$ clusters has already been discussed up to $n = 6$.[10] The electronic spectra of these small, collisionally cooled, clusters were dominated by the coexistence of distinct structural isomers, whose characteristic shifts could be rationalized by using the site specific shift additivity rule. Above $n = 6$ the identification of structural isomers is no longer possible, as a consequence of both the number of such isomers and the transition to the regime where evaporative cooling dominates. For $n = 8$ and 9 the first moment red-shift is reduced almost to zero, indicating that isomers involving structures of the "$-NH_2$ site" type should contribute. This present work focuses on larger clusters ($n \geq 10$) for which three regimes can be identified. Up to $\approx$13 the vdW electronic shift decreases to the red by about 9 cm^{-1} per argon atom. Between $n \approx 13$ and 21 a plateau is observed at about -55 cm^{-1}. For $n \geq 22(\pm 1)$, the red-shift decreases monotonically by only about 3 cm^{-1} per argon atom. It appears clearly that the average strength of the effective interaction of the Ar atoms with the electrons involved in the chromophore transition is much weaker in this last range of size.

B. Ionization Potential. Two sets of mass spectra have been averaged from 2000 laser counts. The second wavelength was varied to build the photoionization efficiency curves. From $n = 6$ to 20 and 20 to 35, the energy of the ionizing photon was decreased by successive steps of 100 and 50 cm^{-1}, respectively (the wavelength of the $S_1 \leftarrow S_0$ excitation photon was separately optimized). The ionization efficiency curves were built from the calculation of the area of the mass peaks for every photon energy. From the positions of the onsets in these curves, the vertical IP of the different vdW clusters has thus been determined. In Figure 3, the shift of the IP relative to the monomer's IP has been plotted versus the number of argon atoms.

As a function of size three regimes are clearly identified ($n \lesssim 12$, $12 \lesssim n \lesssim 22$, and $n \gtrsim 22$). These regimes are approximately linear. From $n = 6$ to 12, the decrease per argon atom is about 180 cm^{-1}, from $n = 12$ to 22 about 90 cm^{-1}, and

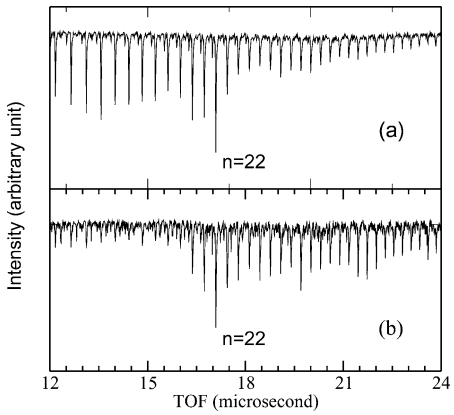

Figure 4. Resonant two-photon two-color ionization mass spectra obtained with two different values of λ_2: (a) λ_2 is set to just above the ionization potential of the aniline−Ar_6 cluster and (b) λ_2 is set to just above the ionization potential of the aniline−Ar_{16} cluster. The residual signal due to one color ionization can be seen in part b.

for $n \gtrsim 22$ it falls to 24 cm^{-1}. These identified regimes are consistent with those obtained for the $S_1 \leftarrow S_0$ electronic transition.

C. Mass Spectra. Two selected mass spectra are shown in Figure 4. They were obtained at two different ionizing photon energies to minimize the excess energy in the ions (see caption). The intensity of the $n = 22$ cluster peak is prominent in both spectra. In particular it is found to be much higher than the $n = 23$ peak in both cases. This "magic" behavior was also observed when using different gas mixtures, from a pure argon expansion to an An/Ar mixture diluted in helium. This allowed the flight-time of neutrals in the molecular beam to be changed and the effects of the evaporative cooling on the neutral distribution in the 200−500 μs range to be explored. It reveals that the aniline−Ar_{22} cluster is a magic number in the R2P2CI mass spectra. In a one-color scheme ($\approx$9000 cm^{-1} above the ionization threshold for $n \geq 22$) this magic number already has been observed and a difference in the survival probability of the cations (the ratio between the peak intensity of the parent and daughter clusters measured in the mass spectra obtained in a reflectron-TOF mass spectrometer) has been inferred for clusters larger than $n = 22$.[33]

According to the spectroscopic results this "magic" character of $n = 22$ cannot be the consequence of an optical selectivity due to the size evolution of the spectroscopic features (vdW shift and bandwidth) of the $S_1 \leftarrow S_0$ electronic transition for the large clusters. Different interpretations can be given since, as is often the case for this kind of observation, the magic character may reflect either the neutral cluster distribution or a particular stability of the ionic cluster. In addition changes between the neutral and ionic cluster conformations can be present and moreover may vary with size. This may lead to a difference in the vibrational energy injected into the ions following the ionization step, thus affecting the ionic fragmentation dynamics at given sizes.

V. Theoretical Predictions and Discussion

A. Binding Energies and Structures. The structure and binding energy (BE) of the most stable isomer for the neutral aniline−Ar_n clusters were calculated from two sets of 7000 quenches for each cluster size between $n = 7$ and 25. The initial conditions for the quenches have been generated from a trajectory at a kinetic temperature $T \approx 30$ K, which allows exploration of a large volume of the configuration space without any dissociation of the cluster during the MD simulation.

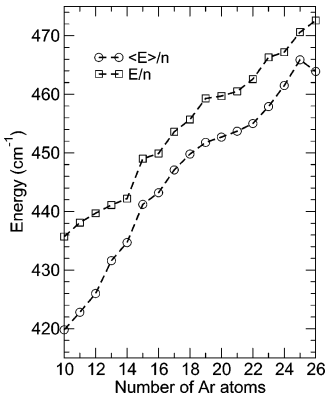

Figure 5. Binding energies per argon atom of the aniline−Ar_n neutral clusters as a function of n. The squares correspond to the absolute minimum energy structures. The circles give the mean binding energy averaged over the structural isomer probability distribution (see text).

In Figure 5 the BE per argon atom of the most stable structure, noted E/n, is reported as a function of cluster size. Three regimes, characterized by a monotonic increase of E/n versus n, can be identified in this curve and the slope changes are found around $n = 14$ and 20. For $n < 14$, the value of the localization parameter S_x in the most stable isomer is around 0 Å, indicating that the Ar atoms preferentially interact with the aromatic ring. Between $n = 14$ and 20, S_x is shifted to large positive values, implying a displacement of the Ar_n cluster toward the amino group. In this size range, S_x/n is approximately equal to 2 Å. When $n \geq 21$, S_x/n is slightly negative. These regimes are found to be consistent with the evolution of E/n. They reflect the balance between the aniline−Ar and Ar−Ar interactions: for $n < 14$ the aniline−Ar interaction strongly influences the structure while for larger clusters the Ar−Ar interaction starts to play an important role. Bridged structures are found in the vicinity of the $-NH_2$ site in clusters up to $n = 20$ and on the ring (S_x slightly negative) for clusters larger than $n = 20$. This structural change around $n = 20$ is the consequence of the strongest "ring"−Ar interaction with respect to the "$-NH_2$"−Ar interaction. However, no particularly large stability is found for $n = 22$.

The ensemble-averaged BE $\langle E \rangle$ of a given cluster size also has been calculated:

$$\langle E \rangle = \frac{1}{N_q} \sum_{i=1}^{N_q} E_{min}^{(i)} \qquad (5)$$

in which N_q corresponds to the number of quenches and $E_{min}^{(i)}$ is the BE of the ith local minimum. In Figure 5, $\langle E \rangle/n$ has been reported for $n = 10-26$ with E/n (absolute minimum). The evolution of $\langle E \rangle/n$ is slightly different from that of E/n below $n = 14$. The large "accident" between $n = 14$ and 15 is largely reduced by averaging over all the visited isomers. For $n > 14$, the curves E/n and $\langle E \rangle/n$ versus n seem almost parallel. However, the change of the slope appears now at $n = 22$ and it is reinforced. The energy of the local minima of aniline−Ar_{22} found along a quenching trajectory is plotted in Figure 6a as a function of the S_x parameter. Many of these isomers have configurations with S_x about 30−40 Å although the absolute minimum is located at S_x about −20 Å. In addition many are characterized by a BE very close to that of the most stable isomer. In Figure 6b, the number of minima found in a given energy slice has been reported. Numerous local minima reached during the quenching trajectory are characterized by a BE up to 200−300 cm^{-1} above the absolute minimum energy. More-

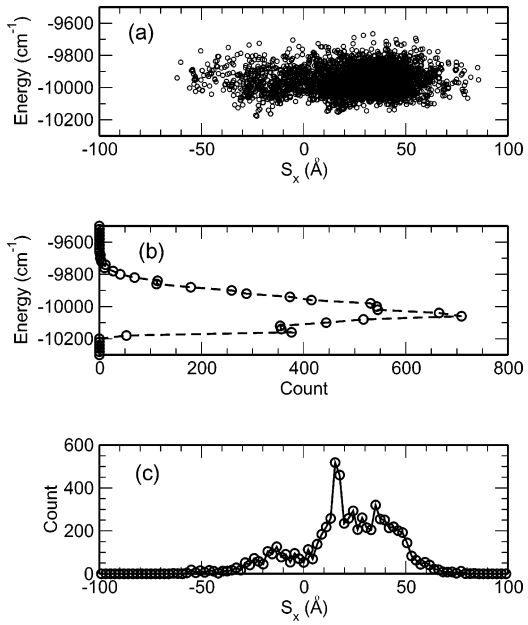

Figure 6. Analysis of the topology of the aniline−Ar_{22} potential energy surface from the outcome of 7000 quenches along a microcanonical trajectory with $T \approx 30$ K. (a) Minimum energy of the local minima as a function of the S_x parameter; (b) number of minima found in a given energy slice; (c) number of minima found in a given slice of S_x values. See the text for the definition of the geometrical parameter S_x.

over configurations with an energy of about 100 cm^{-1} above the global minimum are numerous and so must play an important role in the dynamics. In Figure 6c, the histogram of counts versus S_x is shown. It reveals that many explored isomers are located at large positive values of S_x.

Taking into account the most stable isomer only can be misleading and would be meaningful only if one particular isomer is significantly more stable than the other ones. For the aniline−Ar_n clusters, many isomers are found with an energy comparable to that of the most stable conformation. These conclusions obtained for $n = 22$ are general and can be extended to all the clusters around $n = 20$. Consequently, the global minimum for the neutral clusters cannot be used to explain the spectroscopic data and the mass spectra. This indicates that temperature effects have to be analyzed.

B. Isomerization Dynamics and Its Relation to Spectroscopy. *1. Finite Temperature: How To Characterize the Isomer Distribution?* The temperature, resulting from the evaporative cooling, was predicted from the calculation of evaporation rates to be about 25 K in the size range of about 20 Ar atoms.[34] If the cluster is liquidlike at this temperature, the isomerization dynamics will govern the exploration of the configuration space of the cluster. On the other hand, if the cluster is solidlike, the properties will be governed by the branching ratios between isomers in the last evaporation event. The melting temperatures have thus been evaluated.

For the aniline−Ar_{14} cluster, the melting temperature has been found at approximately $T_{melt} = 18$ K. Around the cluster size $n = 22$, the isomerization dynamics has been precisely analyzed due to the specificity of the aniline−Ar_{22} cluster. In Figure 7, δ_{Ar-Ar}, δ_{An-Ar}, and the kinetic temperature T have been reported as a function of the cluster energy for $n = 21$ and 22. These curves show that the solid−liquid transition occurs nearly at the same temperature, i.e. around $T = 20$ K. It appears that in the experimental conditions T_{melt} is always smaller than that of the sampled clusters. They are liquidlike when they are probed, thus the isomerization dynamics has been investigated for

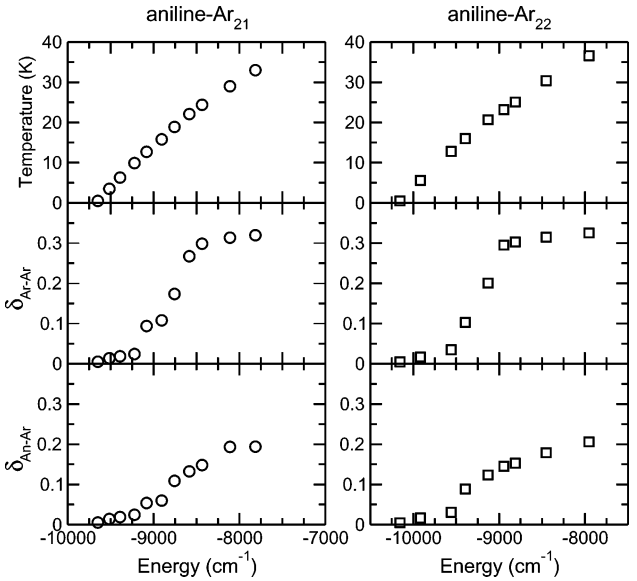

Figure 7. Analysis of the isomerization dynamics in $n = 21$ and 22 clusters as a function of total energy: the top frames show the caloric curve and the middle and bottom frames show the normalized fluctuation of the distance parameters δ_{Ar-Ar} and δ_{An-Ar}.

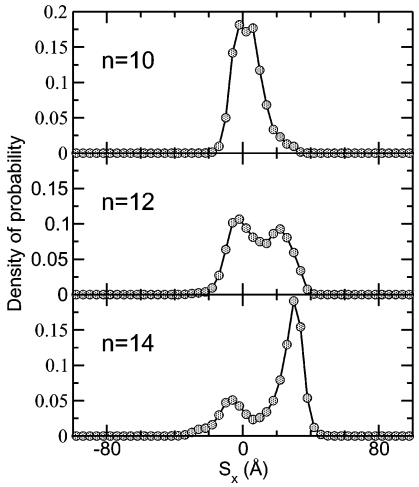

Figure 8. Density of probability of the S_x parameter along a microcanonical trajectory at $T \approx 30$ K for $n = 10$, 12, and 14.

different cluster sizes to understand the solvation dynamics of the Ar atoms around the aniline molecule at a temperature close to that of a supersonic jet.

2. Isomerization Dynamics for n = 10−16. To obtain information on the evolution of the solvation structure as a function of the energy, the S_x parameter has been calculated during long constant energy trajectories and extracted at constant intervals, every 400 fs. The probability distribution of S_x, $P(S_x)$, has been calculated for $n = 10$, 12, and 14 along trajectories at $T \approx 30$ K. The $P(S_x)$ curves are reported in Figure 8. For $n = 10$, $P(S_x)$ is unimodal and peaks around $S_x = 0$ Å. Due to the relatively small size of the cluster, the interaction between the Ar atoms and the chromophore is favored in configurations for which the Ar atoms interact mainly with the delocalized π electrons. For $n = 12$, $P(S_x)$ presents now two extrema for $S_x \approx 0$ and 20 Å. It indicates that the aniline−Ar_{12} spends almost half of the simulation time in a configuration for which the Ar atoms are strongly influenced by the substituent group. For $n = 14$, $P(S_x)$ has only one maximum but for $S_x \approx 30$ Å. The cluster is now most of the time in a configuration interacting preferentially with the $-NH_2$ group.

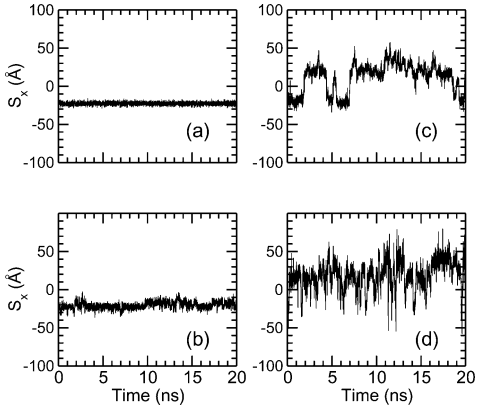

Figure 9. Time evolutions of the S_x parameter in aniline−Ar_{22} along a single microcanonical trajectory at different kinetic temperatures: (a) $T = 13$ K; (b) $T = 20$ K; (c) $T = 25$ K; and (d) $T = 33$ K.

Between $n = 10$ and 14 a net change is also observed for the $P(S_y)$ probability distribution. For $n = 10$, this distribution is bimodal: the two maxima are obtained for ±18 Å. Around $n = 12$, $P(S_y)$ progressively tends to a unimodal distribution centered at $S_y = 0$ Å. It indicates that the cluster spends most of the time in bridged structures, in which the Ar atoms are around the ring for $n < 12$ and around the $-NH_2$ group for $n > 12$. In addition these clusters are always in wetting structures. For $n = 15$ and 16 the behavior is very similar to that for $n = 14$.

3. Isomerization Dynamics for n = 17−24. Around the cluster size $n = 22$, the isomerization dynamics has been analyzed in more detail due to the specificity of the aniline−Ar_{22} cluster. In Figure 9, the time evolution of S_x for $n = 22$ along 20 ns trajectories is reported for values of the energy corresponding to kinetic temperatures $T = 13$ (panel a), 20 (panel b), 25 (panel c), and 33 K (panel d). It shows a strong entropic effect: the basins visited in the PES change dramatically as a function of the energy deposited in the cluster. At $T = 13$ K, the cluster vibrates around its absolute minimum energy configuration: the S_x value exhibits small oscillations around ≈−22 Å. At $T = 20$ K, the amplitude of this motion becomes larger but the S_x parameter remains in the same range of values. The cluster can isomerize but the system is always located in the same basin of the PES. At $T = 25$ K the dynamics is totally changed, as is apparent from the steps in the time evolution of S_x: the cluster explores more and more isomers, and in particular isomers in which Ar atoms are located around the $-NH_2$ group. At $T = 33$ K the cluster now spends most of the time with $S_x \approx 25-30$ Å, indicating that the local entropy favors the presence of Ar atoms in the vicinity of the $-NH_2$ group. This is consistent with the fact that most of the quenches are found with $S_x \approx 30-35$ Å (see Figure 6a).

In Figure 10, the probability distribution $P(S_x)$ has been plotted for the aniline−Ar_n clusters between $n = 17$ and 24. A net change is found as a function of the cluster size: for $n \leq 20$, the distribution is strongly peaked around $S_x \approx 30$ Å with a small bump near $S_x = -20$ Å, which is similar to that for $n = 14$. For $n = 21$ and 22 the distribution is always peaked around positive values of S_x but a double peak structure takes place around $S_x = 20$ and 30 Å. For $n > 22$ a strong change appears and the distribution now peaks around $S_x \approx 0$ Å. It indicates a solvation mostly centered near the center of the aromatic ring. The same trend was observed for colder clusters at $T \approx 25$ K, which is the approximate temperature of the product cluster in the last evaporation event, i.e. the temperature of the probed clusters. In this case, the distributions have been

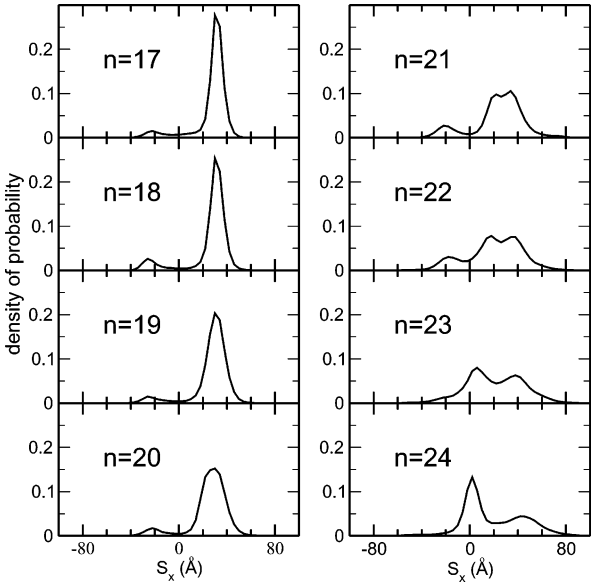

Figure 10. Density of probability of the S_x parameter along single microcanonical trajectories at $T \approx 30$ K for $n = 17-24$. Note the change of pattern between $n = 22$ and 23.

evaluated from longer trajectories (400 ns) to keep the statistical significance despite the lowering of the isomerization rates.

Whatever the cluster size is, the $P(S_y)$ curves remain unchanged: the mean value of S_y is around 0 Å, the distribution is maximum for $S_y = 0$ Å, and the full width at half-maximum (fwhm) of these distributions is typically 20−30 Å. On the contrary the distribution of the S_z parameter does experience some changes as a function of the number of Ar atoms. For $n \lesssim 18$, the S_z parameter is distributed around 0 Å with a typical fwhm equal to 10 Å. For $\gtrsim 18$, the distributions are mainly peaked around 0 Å with two minor contributions at $S_z = \pm 30$ Å. Between $n = 18$ and 22, the solvation structure remains favored in the vicinity of the $-NH_2$ substituent but the Ar atoms begin to explore configurations in which some Ar atoms are located at a large distance from the chromophore plane. Large values of S_z are reached but only when the center of mass of the argon atoms is mostly displaced to large positive values of S_x. It is noteworthy that wetting structures remain the most probable whatever the cluster size is.

4. Outline of Average Structural Changes. In brief the cluster structures which dominate the probability distribution are then the following: bridged wetting structures with argon atoms in an incomplete first solvation shell from $n = 10$ to 17; appearance of nonwetting structures from $n = 18$, which are localized near the amino group; and ring-*centered* wetting structures above $n = 22$.

Additionally it can be noted that the bridging atoms tend to bind to the peripheral hydrogen atoms of the ring for $n = 10$ to 12 and for $n > 22$, and to the amino group for $n = 13$ to 22. Note that in this paper, following the terminology cast by Solcà and Dopfer,[23] we use the expression "H-bound" cluster only in the last case, where some argon atoms interact preferentially with the two hydrogen atoms of the amino group. From the electronic point of view the orbitals on nitrogen participate in this binding.

C. Neutral Solvation Structure and Its Relation to Spectroscopy. The isomerization dynamics has revealed that the localization parameter S_x is the pertinent solvation coordinate to characterize the spectroscopic regimes. On the basis of spectroscopic data for small cluster sizes,[6,10,23] it is interesting to check if the size evolution of the electronic shifts might be

explained by an average solvation structure (π-bound and H-bound structures). The $S_1 \leftarrow S_0$ electronic transition for the small clusters has revealed a blue-shift when the Ar atoms are located in the vicinity of the amino group and a red-shift when the Ar atoms interact with the ring.[6,10] The evolution of the $S_1 \leftarrow S_0$ electronic shift around $n = 12$ and 22 is consistent with such a behavior: between $n = 13$ and 22 the stabilization in the S_1 state with respect to S_0 is weaker for these H-bound clusters than in the π-bound ones, $n < 12$ and $n > 22$ (see Figure 2). For large clusters ($n \geq 22$) the electronic shift is weakly dependent on the cluster size probably reflecting the Ar shell closure around the chromophore.

For the small clusters, the electronic shift of the IP was also shown to be dependent on the Ar localization around the chromophore characterized by a larger red-shift from the NH_2-binding site.[35,36] For large clusters, the slope of the IP versus the cluster size is maximal in the $n = 6$ to 10 interval, in agreement with the role of argon atoms interacting with the amino group. It is then reduced around $n = 12$ (see Figure 3). It is certainly the consequence of the change in thermal-averaged structure in the neutral ground electronic state as predicted in section B. For $n \geq 22$ the IP shift is weakly dependent on the cluster's size as is the $S_1 \leftarrow S_0$ electronic transition shift, due to the previously mentioned first Ar shell closure around the chromophore.

D. Neutral Solvation Structure and Its Relation to Ionic Clusters Dynamics. Mass spectrometry is recognized in cluster science as a powerful technique to study the stability of ionic clusters.[37−43] For the neutrals, when ionization and heating processes are not separately controlled, peak intensity in the mass spectra does not automatically reflect the stability of a particular mass. An interpretation of "anomalous" large intensities in a mass spectra is thus not trivial. In the framework of the Franck−Condon approximation, the amount of internal energy injected into the ionic cluster is linked to the degree of geometrical change between the neutral and ionic species. We could easily imagine that for a peculiar atomic or molecular cluster, the internal energy in the ions will be dependent on the cluster's size. This would induce a strong size dependence of the ionic cluster dynamics.

On this basis, we can now analyze the consequence of the isomerization dynamics in the neutral species around $n = 12$ and 22 on the ionization step. Recent experimental and ab initio data on the ionic aniline$^+-Ar_{1,2}$ indicate that the H-bound structure is more stable than the π-bound structure in the ground ionic electronic state.[23] The infrared spectra of the NH_2 stretching mode in aniline$^+-Ar_n$ ($n = 1-21$) ionic clusters have also been collected.[22] The ions were prepared through a R2PI scheme. One interesting feature observed in this experiment is that the bandwidth decreases monotonically from 6 cm^{-1} for $n = 8$ down to 2 cm^{-1} for $n = 12$. When $n \geq 12$, the bandwidth is almost constant. It most probably indicates that the temperature of the ionic clusters is decreasing up to $n = 12$ and keeps a constant value for larger clusters. Because the ionization process is vertical, it provides a contribution to the vibrational energy injected in the cations. As the bandwidth narrows, this contribution is found to decrease with size up to $n = 12$. The vibrational dynamics in S_0 has shown that H-bound clusters are the averaged structures in S_0 for $n = 12-22$, and it indicates that the D_0 ionic ground state also has this averaged structure in this range of sizes. Below $n = 12$, the heating of the ionic cluster reveals that the H-bound cluster remains the averaged structure in D_0. This is consistent with the calculated geometry of the aniline$-Ar_{1,2}$ cations.

Some years ago, the evaporation dynamics of the ionic aniline$-Ar_n$ clusters had been investigated by Guillaume et al.[33] using a reflectron-type mass spectrometer. The ionic species were prepared via a one-color two-photon ionization process and a "magic" number was found for $n = 22$. Indeed for $n > 22$, the survival probability of the ionic cluster was found to strongly decrease.[33] This feature had been interpreted in terms of a dynamical closure of the first Ar solvation shell around the chromophore (wetting structure) in the cation. In light of the isomerization dynamics characterized in our present work, a new interpretation of this magic number can be proposed. Between $n = 12$ and 22, a small amount of vibrational energy is injected in the ionic species while for $n \geq 22$ the neutral averaged geometry is modified (Ar atoms are now around the ring). Thus the decrease of the survival probability could be a direct consequence of the increase of the vibrational energy deposited in the cation. This would indicate that the averaged geometry in the ionic cluster remains unchanged in this range of sizes, i.e. the Ar atoms are located around the amino group.

As a final remark, it should be recalled that the possible contribution to the "magic" character observed for $n = 22$ resulting from the evaporation dynamics in neutral clusters has not been evaluated, although the change of regime found at this particular size in the isomerization dynamics might have an influence on the evaporation rate.

VI. Conclusion

Thanks to a combined study of the aniline$-Ar_n$ clusters with both experimental and theoretical appropriate tools, the present work has brought a very significant advance in the understanding of solvation dynamics in finite temperature clusters. Spectroscopic data have been recorded for large aniline$-Ar_n$ clusters. The electronic vdW shift and vertical ionization potential have been measured as a function of cluster size, from $n = 8$ up to 35. From these experimental data, three regimes have been identified and understood from MD simulations as consequences of the isomerization dynamics in S_0. The shifts of the $S_1 \leftarrow S_0$ transition as well as the ionization potential as a function of cluster size have been explained in terms of average solvation structures, governed by the competition between the solvent−solvent and solute−solvent interactions. The role of temperature on well-defined structural parameters has been investigated in detail by molecular dynamics simulations in large vdW clusters, so that the signature of the solvation dynamics was inferred on the spectroscopic observables. In particular the important role of wetting structures involving argon atoms in the vicinity of the amino group is clearly recognized in the spectral shift curves for the size interval $n = 13$ to 22.

This analysis led also to the conclusion that large ionic aniline$^+-Ar_n$ clusters possess H-bound structures so that for $n > 22$, due to the change in the neutral average structure, the injected vibrational energy increases with size in a one-color two-photon ionization scheme. As a general conclusion, we have shown that the solvation dynamics at finite temperature has to be taken into account to interpret the experimental results on clusters, even in weakly bound vdW clusters, as soon as they are subject to evaporative cooling.

References and Notes

(1) Schlag, E. W., Weinkauf, R., Miller, R. E., Eds. Molecular clusters. In *Chem. Phys.* **1998**, *239*, 1.

(2) Brutschy, B., Hobza, P., Eds. van der Waals, III. In *Chem. Rev.* **2000**, *100*, 3861.

(3) Leutwyler, S.; Bösiger, J. *Chem. Rev.* **1990**, *90*, 489.

(4) Shalev, E.; Ben-Horin, N.; Even, U.; Jortner, J. *J. Chem. Phys.* **1991**, *95*, 3147.
(5) Bieske, E. J.; Uichanco, A. S.; Rainbird, M. W.; Knight, A. E. W. *J. Chem. Phys.* **1991**, *94*, 7029.
(6) Hermine, P.; Parneix, P.; Coutant, B.; Amar, F. G.; Bréchignac, Ph. Z. *Phys. D* **1992**, *22*, 529.
(7) Zhang, X.; Smith, J. M.; Knee, J. L. *J. Chem. Phys.* **1992**, *97*, 2843.
(8) Takahashi, M.; Ozeki, H.; Kimura, K. *J. Chem. Phys.* **1992**, *96*, 6399.
(9) Parneix, P.; Halberstadt, N.; Bréchignac, Ph.; Amar, F. G.; van der Avoird, A.; van Bladel, J. W. I. *J. Chem. Phys.* **1993**, *98*, 2709.
(10) Douin, S.; Parneix, P.; Amar, F. G.; Bréchignac, Ph. *J. Phys. Chem.* **1997**, *101*, 122.
(11) Jäckel, J. G.; Jones, H. *Chem. Phys.* **1999**, *247*, 321.
(12) Hineman, M. F.; Kelley, D. F.; Bernstein, E. R. *J. Chem. Phys.* **1993**, *99*, 4533.
(13) Grégoire, G.; Dedondeur-Lardeux, C.; Jouvet, C.; Martranchard, S.; Solgadi, D. *J. Phys. Chem. A* **2001**, *105*, 5971.
(14) Miyazaki, M.; Fujii, A.; Ebata, T.; Mikami, N. *Chem. Phys. Lett.* **2001**, *349*, 431.
(15) Miyazaki, M.; Fujii, A.; Ebata, T.; Mikami, N. *Phys. Chem. Chem. Phys.* **2003**, *5*, 1137.
(16) Solcà, N.; Dopfer, O. *J. Phys. Chem. A* **2003**, *107*, 4046.
(17) Dessent, C. E. H.; Geppert, W. D.; Ullrich, S.; Müller-Dethlefs, K. *Chem. Phys. Lett.* **2000**, *319*, 375.
(18) Dedondeur-Lardeux, C.; Grosswasser, D.; Jouvet, C.; Martranchard, S.; Teahu, A. *Phys. Chem. Chem. Phys.* **2001**, *3*, 4316.
(19) Solcà, N.; Dopfer, O. *J. Phys. Chem. A* **2001**, *105*, 5637.
(20) Nakanaga, T.; Ito, F.; Miyawaki, J.; Sugawara, K.; Takao, H. *Chem. Phys. Lett.* **1996**, *261*, 414.
(21) Piest, H.; von Helden, G.; Meijer, G. *J. Chem. Phys.* **1999**, *110*, 2010.
(22) Nakanaga, T.; Ito, F. *Chem. Phys. Lett.* **2002**, *355*, 109.
(23) Solcà, N.; Dopfer, O. *Eur. Phys. J. D* **2002**, *20*, 469.
(24) Douin, S.; Fillion, J. H.; Bonneau, M.; Bréchignac, Ph.; Furio, D.; Gauyacq, D.; Horani, M.; Shafizadeh, N. *Chem. Phys. Lett.* **1993**, *216*, 215.
(25) Evans, D. J. *Mol. Phys.* **1977**, *34*, 317. Evans, D. J.; Murad, S. *Mol. Phys.* **1977**, *34*, 327.
(26) Lindemann, F. A. *Phys. Z.* **1910**, *11*, 609.
(27) Knochenmuss, R.; Ray, D.; Hess, W. P. *J. Chem. Phys.* **1994**, *100*, 44.
(28) Zhang, X.; Pitts, J. D.; Nadarajah, R.; Knee, J. L. *J. Chem. Phys.* **1997**, *107*, 8239.
(29) Troxler, T.; Leutwyler, S. *J. Chem. Phys.* **1991**, *95*, 4010.
(30) Bahatt, D.; Heidenreich, A.; Ben-Horin, N.; Even, U.; Jortner, J. *J. Chem. Phys.* **1994**, *100*, 6290.
(31) Ben-Horin, N.; Bahatt, D.; Even, U.; Jortner, J. *J. Chem. Phys.* **1992**, *97*, 6011.
(32) Brand, J. C. D.; Jones, V. T.; Forrest, B. J.; Pirkle, R. J. *J. Mol. Spectrosc.* **1971**, *39*, 352.
(33) Guillaume, C.; Le Calvé, J.; Dimicoli, I.; Mons, M. *J. Phys. Chem.* **1994**, *98*, 13443.
(34) Parneix, P.; Amar, F. G.; Bréchignac, Ph. *Chem. Phys.* **1998**, *239*, 121.
(35) Douin, S.; Hermine, P.; Parneix, P.; Bréchignac, Ph. *J. Chem. Phys.* **1992**, *97*, 2160.
(36) Douin, S.; Piccirillo, S.; Bréchignac, Ph. *Chem. Phys. Lett.* **1997**, *273*, 389.
(37) Märk, T. D.; Scheier, P.; Leiter, K.; Ritter, W.; Stephan, K.; Stamatovic, A. *Int. J. Mass Spectrom. Ion Processes* **1986**, *74*, 281.
(38) Echt, O.; Kandler, O.; Leisner, T.; Miehle, W.; Recknagel, E. *J. Chem. Soc., Fraraday Trans.* **1990**, *86*, 2411.
(39) Wei, S.; Shi, Z.; Castelman, A. W., Jr. *J. Chem. Phys.* **1991**, *94*, 8604.
(40) Bréchignac, C.; Cahuzac, Ph.; Leygnier, J.; Weiner, J. *J. Chem. Phys.* **1989**, *90*, 1492.
(41) Haberland, H.; Kornmeier, H.; Langosch, H.; Oschwald, M.; Tanner, G. *J. Chem. Soc., Faraday Trans.* **1990**, *86*, 2473.
(42) Jarrold, M.; Honea, E. *J. Phys. Chem.* **1991**, *95*, 9185.
(43) Martin, T. P.; Bergmann, T.; Göhlich, H.; Lange, T. *Chem. Phys. Lett.* **1990**, *172*, 209.